ORIGINAL PAPER

Sulfide-enhanced electrochemical capacitance of cobalt hydroxide on nanofibered parent substrate

Svetlana Lichušina · Ala Chodosovskaja ·
Konstantinas Leinartas · Algirdas Selskis ·
Eimutis Juzeliūnas

Abstract Two approaches—substrate nanostructuring and incorporation of sulfide—were studied with the aim to increase electrochemical capacitance of cobalt (hydro) oxide. A fiber structure of cobalt was deposited electrochemically with the fibers in the order of tens of nanometers in thickness and hundreds of nanometers in length. Cobalt hydroxide film was formed on the nanostructured substrate by anodic polarization in an alkaline solution. The hydroxide formation and its electrochemical capacitance have been studied by cyclic voltammetry in conjunction with the electrochemical quartz crystal microbalance (EQCM). An irreversible behavior was typical of the first anodic polarization cycle; it turned gradually to a reversible one during subsequent cycling. EQCM measurements indicated exponential electrode mass growth during the first cycle, with subsequent transition to a quasipassive state. The redox transitions Co(II)→Co(III)→Co(IV), which determine pseudocapacitance, did not cause remarkable electrode mass change. The electrochemical capacitance of the nanofiber sample was found up to five times higher when compared to that formed on conventional cobalt (abraded surface). Specifics of "per 1 g" evaluation of capacitance performance is discussed. Measurements showed that about 10% of the entire hydroxide structure took part in the capacitive process. The capacitance value determined per 1 g of active $Co(OH)_2$ was in agreement with the limiting value predicted by the Faraday's law (2,421 F g^{-1}) sulfide-enhanced system with 18% CoS exhibited up to three times higher capacitance when compared to that of the sulfide-free counterpart. The system shows promise for practical applications due to its low cost and technical simplicity.

Keywords Cobalt hydroxide · Cobalt sulfide · Nanostructure · Nanofiber · EQCM · Supercapacitors

Introduction

Pseudocapacitance studies of metal oxide films are of increasing importance due to their application for development of electrochemical capacitors (supercapacitors and ultracapacitors) [1, 2]. Ruthenium oxide has been shown to be probably the best electrode material in terms of a high-specific capacitance, a wide potential window, and a long shelf and cycle life [2–6]. However, a critical issue in commercialization of the electrodes is a high cost of ruthenium oxide; therefore, cheaper substitutes are of increasing interest.

Studies of cobalt oxides as an electrode material for supercapacitor applications started around a decade ago [7–10]. Srinivasan and Weidner used the electrochemical precipitation technique, which yielded a specific capacitance about 40 F g^{-1} [7]. A much higher capacitance of ca. 290 F g^{-1} was reported for cobalt oxide xerogel powders prepared by a sol–gel process [8]. Jayashree and Kamath performed synthesis of α-cobalt hydroxide electrochemically by cathodic reduction of a cobalt nitrate and obtained a layered structure with an interlayer spacing of 8.93 Å [9]. Electrochemistry of cobalt oxides has been studied by Liu et al. [10]. The authors came to a conclusion that a Co oxide film, though behaves analogously to RuO_2, has several unfavorable features such as a limited capacitance

S. Lichušina · A. Chodosovskaja · K. Leinartas · A. Selskis ·
E. Juzeliūnas (✉)
Institute of Chemistry,
A. Goštauto 9,
01108 Vilnius, Lithuania
e-mail: ejuzel@ktl.mii.lt

density, a rather short (0.7 V) operable potential window, and a quite nonconstant capacitance within the window.

Significant efforts were undertaken to create cobalt (hydro)oxide systems with a superior capacitance performance [11–24]. Cobalt oxide films were formed from electrochemically precipitated hydroxide by thermal conversion to Co_3O_4 in air [11]. The authors showed adequate capacitance and wide electrochemical window for asymmetric capacitor consisting of NiO_x positive electrode and Co_3O_4 negative one.

Deposition of thin films of Co_3O_4 by spray pyrolysis was studied by Shindle et al. [12]. The films were deposited on glass substrates from cobalt chloride solutions. The authors report the specific capacitance value of 74 F g^{-1}.

Physical techniques of cobalt oxide formation have also been applied [13]. The films were obtained by radio frequency sputtering at different gas composition (O_2, Ar). The electrochemical properties of the films were examined using the system denoted as all solid-state thin film supercapacitors, which consisted of Co_3O_4 and an amorphous LiPON thin film electrolyte.

Effects of complexing agents (acetate, citrate, and ethylenediaminetetraacetic acid) were studied on the properties of cobalt oxides obtained by anodic deposition [14]. Highest specific capacitance of 230 F g^{-1} was determined for the oxide deposited from the solution containing acetate ions.

Cobalt oxide film was deposited onto copper substrate from cobalt chloride precursor at a room temperature [15]. The maximum specific capacitance was found of such film 165 F g^{-1} in 1.0 M KOH at10 mV s^{-1}.

A few research groups recently studied cobalt oxides/hydroxides applied to nanosized structures. A composite material consisting of $Co(OH)_2$ on ultra-stable Y zeolite molecular sieves was prepared by Cao et al. [16]. The maximum specific capacitance of 1,492 F g^{-1} was obtained, which according to the authors, is the highest one reported for supercapacitors. A mesoporous nanocrystalline Co_3O_4 was deposited from a gel-floccules system, mixing the oxide with conducting graphite and forming a composite layer onto the nickel substrate [17]. The material exhibited a specific capacitance of ca. 400 F g^{-1}. The CoOOH nanoflake films were formed on nickel by immersing the substrate into methanol/water mixed solution of cobalt acetate and subsequent drying at 60 °C [18]. The capacitance value was determined to be around 200 F g^{-1}. Cathodic electrodeposition of cobalt films with a flower-like nanostructure was reported by Nguyen et al. [19]. The authors reported redoxable behavior of the film, though no data were given on the pseudocapacitance of the system.

In recent years, further approaches aimed to achieve improved capacitance performance of cobalt hydroxide have been reported, which include ordered mesoporous films [20, 21], nanosheets with interlayer spacing size close to that of hydrated ions (6–8 Å) [22], and physical vapor deposited parent substrate [23].

Cobalt sulfide is a promising cathode material for lithium rechargeable batteries [24]. A few studies were carried out of the sulfide application as an electrode material for electrochemical supercapacitors [25–27]. The specific capacitance values for CoS_x prepared by chemical precipitation method were determined in the range from 369 to 475 F g^{-1} [25]. CoS nanospheres and nanowires were formed by a biomolecule-assisted process using L-cysteine as the sulfide source and $CoCl_2$ solution with subsequent heating at 190 °C [26]. A specific capacitance of 508 F g^{-1} was achieved for the CoS nanowires.

Synthesis of amorphous nanosized CoS_x was reported recently at H_2O-CS_2 interface using $Co(OOCCH_3)_2$ as a cobalt source [27]. The working electrode for supercapacitance measurements was prepared by pressing CoS_x onto nickel foam. The as-prepared product exhibited poor capacitance performance during the first polarization cycles, whereas high supercapacitance values up to 910 F g^{-1} were obtained after prolonged cycling (240 cycles). Authors came to conclusion that CoS_x nanoparticles gradually transform around their exterior surfaces into $Co(OH)_2$ nanowhiskers.

Our research aims to electrochemically deposit the cobalt hydroxide and hydroxide-sulfide structure of superior capacitance on a nanofiber parent substrate. When compared to chemical methods, electrochemical means provide advantages of relative simplicity, low cost, and easy control of the surface structure and composition. Using of parent metal substrate provides an opportunity to increase cycle life of the capacitor as the disintegrated hydroxide can be recovered during anodic polarization cycles. To the best of our knowledge, this is the first report on supercapacitance properties of electrochemically deposited cobalt sulfide–hydroxide structure.

Experimental

Cobalt coatings with a nanofiber structure were deposited from the electrolyte for Zn-Co alloy electroplating as described in patent [28] with only difference that zinc ions were excluded from the plating bath. The electrolyte was prepared using analytical class purity reagents $CoSO_4 \times 7H_2O$ (20 g L^{-1}), NaOH (100 g L^{-1}), a complexing agent (40 g L^{-1}), and triple distilled water. The coatings were deposited on carbon steel plates (S=1 cm^2), which were pretreated with emery paper (grade 2500) and an MgO powder, rinsed with 5% HCl and finally with distilled water. The electroplating current efficiency determined by microgravimetric measurements was approximately 50%.

Cobalt hydroxide layer was formed electrochemically on the cobalt substrate in 1 M NaOH by applying ten cycles within the polarization interval $E=-1.0$ to 0.6 V at $v=20$ mV s^{-1}.

Cobalt sulfide and cobalt hydroxide composite was formed on the cobalt substrate by applying ten voltammetric cycles at 20 mV s^{-1} within the potential interval $E=-0.3$ to 0.4 V in the solution 10 g L^{-1} Na$_2$S+5 g L^{-1} NaOH. The sample surface was analyzed by X-ray photoelectron spectroscopy. The content of elements (in atomic percentage) was found to be oxygen -27.3%, sulfide -18.5%, and cobalt -52.9%.

A Parstat 2273 potentiostat from Princeton Applied Research Instruments (USA) was used to carry out cyclic voltammetry measurements. A three-electrode cell with platinum foil as a counter electrode and a saturated silver/silver chloride as reference were used. The electrolyte was 1 M NaOH, which was deoxygenated by Ar gas prior to measurements. All the potentials given throughout the paper are against saturated Ag/AgCl electrode.

Electrochemical quartz crystal microbalance (EQCM) measurements were performed using the above potentiostat in conjunction with a microgravimetric unit PAR 922 from Princeton Applied Research Instruments (USA). Quartz discs with a fundamental frequency f_o of 5 MHz were employed. The proportion coefficient of the oscillator between the frequency and the mass change was $K=18$ ng Hz^{-1} cm^{-2}. A sub-layer of iron was sputtered onto quartz discs by a magnetron sputtering technique using the equipment from Leybold Vacuum (Germany).

The surface microtopography was studied by scanning electron microscopy (SEM; EVO 50 EP from Carl Zeiss SMT AG, Germany) with energy dispersive and wave dispersion X-ray spectrometers (Oxford, UK).

The oxide mass was determined by conventional weighing of steel plates ($S=2$ cm^2) after Co plating as described above and applying ten polarization cycles in 0.1 NaOH. The specimen before weighing was rinsed in water and dried 24 h under ambient conditions. All measurements were carried out at room temperature (20 ± 1 °C).

Results and discussion

SEM images in Fig. 1(a, b) show the surface morphology on a sub-micrometer scale of Co deposits formed on a low carbon steel plate (a) and magnetron sputtered Fe (b) which was used for EQCM measurements. The structure consists of randomly distributed nanofibers, which thickness is in the order of tens of nanometers and the length is in the order of hundreds of nanometers. During the prolonged oxidizing-reduction cycles, the fiber-like structure is trans-formed into thicker highly packed cobalt hydroxide hexagonal platelets (c) and (d). The (e) and (f) micrographs show the flake like microtopography of the sulfide-containing deposits.

Cyclic voltammetry (Fig. 2) indicates highly irreversible behavior of the electrode during the initial cycling. A large initial peak followed by much smaller one (around $E_{peak}=0.2$ V) is observed during the first cycle. When the cycling progresses, the behavior turns gradually from irreversible to reversible one and the second peak shifts to potentials ca. 0.0 V. The transition and the peak is attributed to irreversible Co(OH)$_2$ deposition followed by electrochemical formation of CoOOH, which will be discussed in more detail below.

Figure 3 demonstrates a prolonged cycling experiment (selected are the curves for the cycles 11,330 and 1,000). Several distinctive peaks are observed on the curves (A, B, and C). The figure compares cathodic and anodic branches: one can be seen that the cathodic branch is mirrored by an anodic one or vice versa. The current responses around $E_{peak}=0.4$ to 0.5 V increase during the cycling as is evident from the curves for the 11th cycle with those of higher numbers. The data also indicate a high cycle life of the oxide structure, which is important from the point of view of practical application. The curves for the cycles 330 and 1,000 differ negligibly what indicates a good stability performance of the system.

The EQCM measurements reveal the electrode mass effects associated with electrochemical reactions (Fig. 4). The irreversible anodic current peak observed during the first polarization cycle yields an exponential mass growth with a further transition to a quasipassive behavior within a wide potential range (ca. -0.3 to 0.6 V). When reversing the potential scan, the electrode holds the passivity over a wide potential range. The mass gain is observed again at the negative end of the voltmassogram. With the number of cycles, the increase in mass is getting suppressed and approaches some limit ($\Delta m_1 \approx 70$ µg cm^{-2}). Thus, two regions could be distinguished: the negative one ($E=-1.0$–0.0 V), where mass gain could occur, and the positive one ($E=0.0$–0.6 V), where no remarkable mass effects are observed. The first region could be attributed to formation of a cobalt oxide and hydroxide according to the reactions [29, 30]:

$$Co + 2OH^- \rightarrow Co(OH)_2 + 2e^- \qquad (1)$$

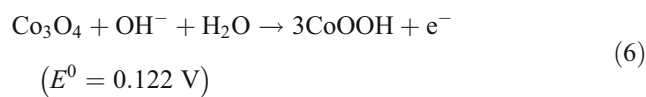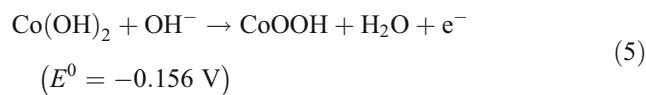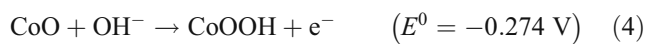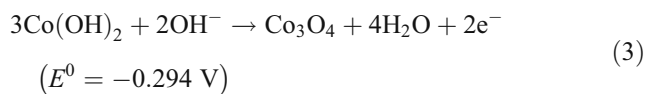$$Co + 2OH^- \rightarrow CoO + H_2O + 2e^- \qquad (2)$$
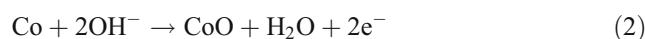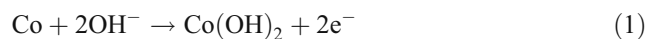
Standard potentials of these reactions at pH 14 are $E^0=-0.918$ V for (Eq. 1) and $E^0=-0.892$ V for (Eq. 2). The first reaction under our conditions is more likely as our measurement relates to highly alkaline medium.

Fig. 1 Scanning electron microscopy (SEM) images of nanofiber structure as deposited cobalt on steel (**a**) and on sputtered iron (**b**) and after the cycling in 1 M NaOH (**c**) and (**d**). SEM images of cobalt sulfide and cobalt hydroxide composite (**e**, **f**)
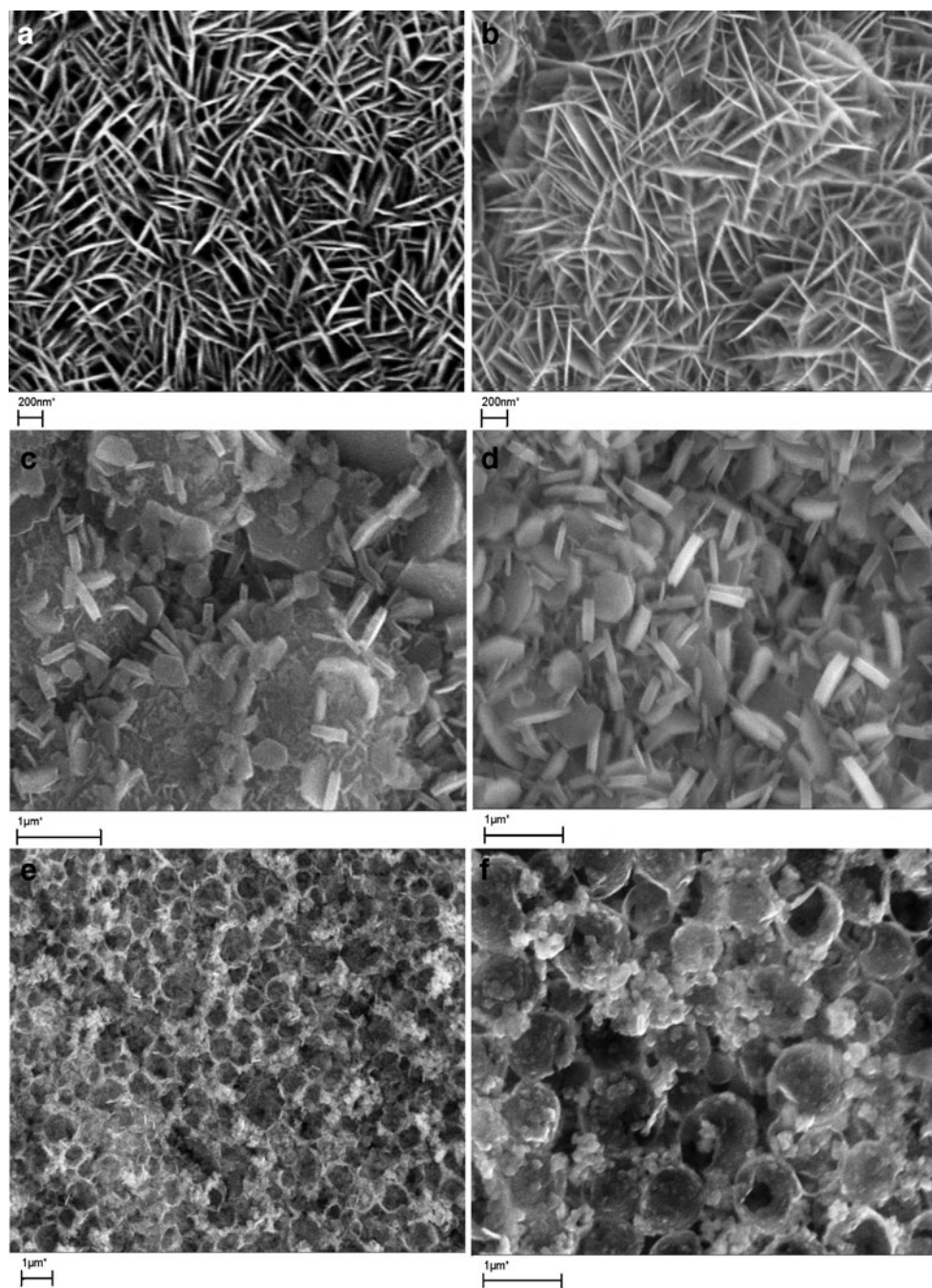
The current peaks A, B, and C, as denoted in Fig. 3, indicate three electrochemical transformations of the (hydro)oxide. Several reactions could be relevant according to their standard potentials [29, 30]:
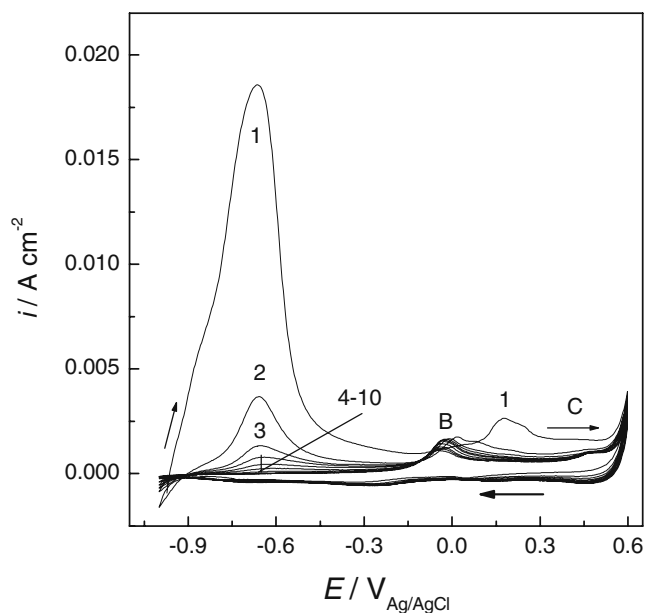
$$3Co(OH)_2 + 2OH^- \rightarrow Co_3O_4 + 4H_2O + 2e^- \quad (3)$$
$$\left(E^0 = -0.294 \text{ V}\right)$$

$$CoO + OH^- \rightarrow CoOOH + e^- \quad \left(E^0 = -0.274 \text{ V}\right) \quad (4)$$

$$Co(OH)_2 + OH^- \rightarrow CoOOH + H_2O + e^- \quad (5)$$
$$\left(E^0 = -0.156 \text{ V}\right)$$

$$Co_3O_4 + OH^- + H_2O \rightarrow 3CoOOH + e^- \quad (6)$$
$$\left(E^0 = 0.122 \text{ V}\right)$$

Fig. 2 Cyclic voltammetry curves for electrochemically deposited cobalt on the steel substrate in 1 M NaOH at a potential scan rate of 20 mV s^{-1}

$$Co(OH)_2 + 2OH^- \rightarrow CoO_2 + 2H_2O + 2e^-$$
$$\left(E^0 = 0.154 \text{ V}\right) \tag{7}$$

$$CoOOH + OH^- \rightarrow CoO_2 + H_2O + e^-$$
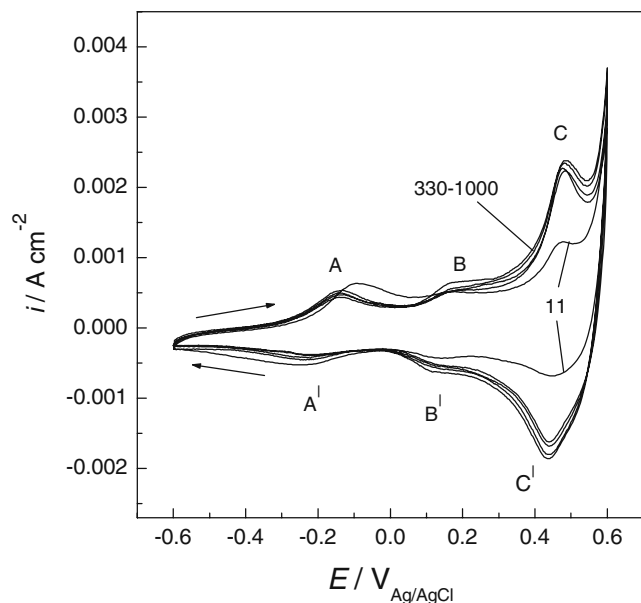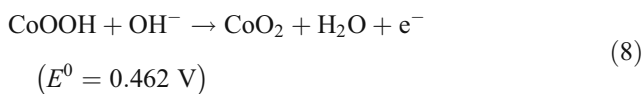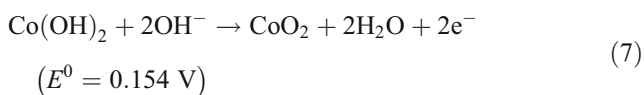$$\left(E^0 = 0.462 \text{ V}\right) \tag{8}$$

Fig. 3 Subsequent cycling of the electrode up to 1,000 cycles following the measurements shown in Fig. 2
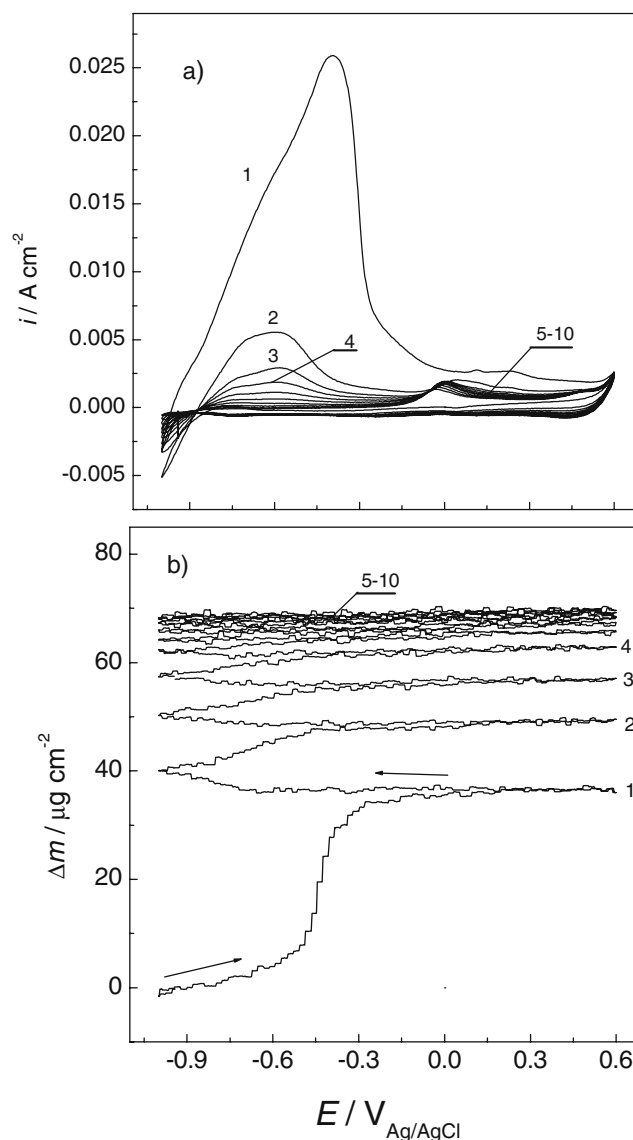

Fig. 4 Electrochemical quartz crystal microbalance and cyclic voltammetry data in 1 M NaOH for electrochemically deposited cobalt. Potential scan rate −20 mV s^{-1}

According to the EQCM data (Fig. 4), the electrochemical transformations indicated by the voltammetric peaks in Fig. 3 are not associated with remarkable mass effects. Thus, the EQCM data allow to elucidate the electrochemical mechanism. Equations 5, 7, and 8, which correspond to the peaks A, B, and C, are most likely as these reactions does not predict significant mass change of the electrode (except of that due to proton release, which is relatively small).

Some comment is necessary concerning the second current peak, which starts around $E=0.1$ V in Fig. 2. This peak is observed only for the first polarization cycle, while it disappears in subsequent cycles (two to ten). Instead, a new peak appears at more negative potentials, $E_{peak} \sim 0.0$ V. The voltmassogram in Fig. 5
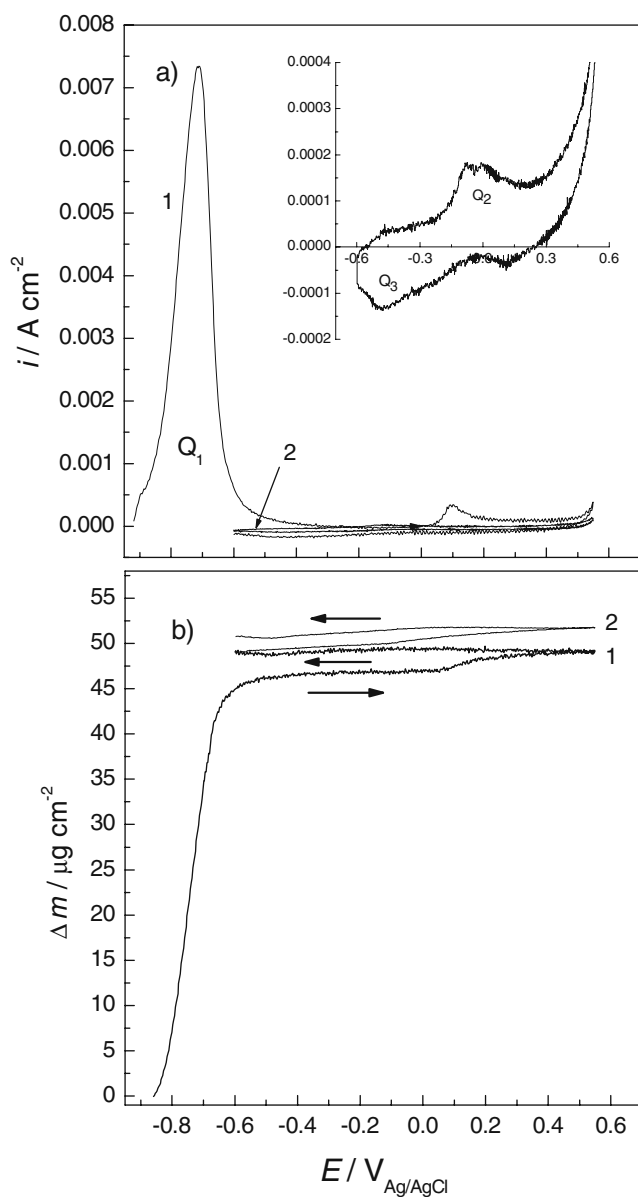
Fig. 5 Electrochemical quartz crystal microbalance and cyclic voltammetry data in 1 M NaOH for electrochemically deposited cobalt. Potential scan rate −2 mV s^{-1}
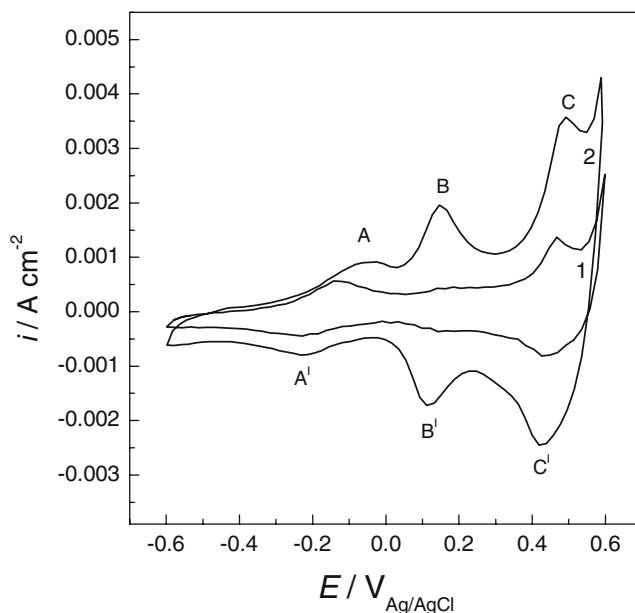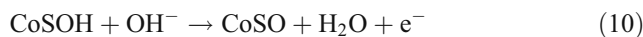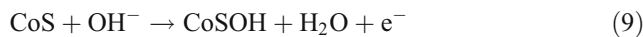

Fig. 6 Cyclic voltammetry curves for electrochemically deposited cobalt on the steel substrate (1) and for cobalt sulfide and cobalt hydroxide composite (2) in 1 M NaOH at a potential scan rate of 20 mV s^{-1}

Thus, the measurements identify three main electrochemical processes: the hydroxide formation by the reaction Co→Co(II) and the subsequent oxidizing stages Co(II)→Co(III)→Co(IV) within the oxide, which determines pseudocapacitance of the system.

Sulfide incorporation into the hydroxide structure leads to appearance of a distinctive current peak at $E=0.1$–0.15 V (Fig. 6). The peak location corresponds to that reported recently in the literature on electrochemical redox behavior of single cobalt sulfide [25, 26]. The mechanism of electrochemical oxidation of cobalt sulfide in alkaline medium remains to be debatable. The authors assumed electrochemical reactions in analogy to those for Co(OH)$_2$ or CoO$_2$, as the potential of electrochemical oxidation of cobalt sulfide is similar to that of the cobalt oxide and oxygen as an element belongs to the same family as sulfur [25, 26]:

$$CoS + OH^- \rightarrow CoSOH + H_2O + e^- \qquad (9)$$

$$CoSOH + OH^- \rightarrow CoSO + H_2O + e^- \qquad (10)$$

It is a common knowledge that the electrochemical capacitance (C), which is due to redox reactions, may be estimated from cyclic voltammetric curves by calculating the charge passed during discharging (the anodic polarization, Q) divided by the potential range in which the curves were recorded (ΔE). It has been found for the sulfide-free hydroxide for 100th cycle capacitance value to be as high as $C \approx 0.03$ F cm^{-2}. It is an important result that the

indicates that the peak under consideration is accompanied by a mass increase ca. 2–3 μg cm^{-2}. This implies Eq. 6, i.e., the transition Co$_3$O$_4$→3CoOOH, whose standard potential is $E^0=0.122$ V, and the electrode mass is increased due to attachment of two additional oxygen atoms and one proton. During the backwards scanning, the CoOOH is converted rather to Co(OH)$_2$ than to Co$_3$O$_4$, so that Eq. 6 is getting suppressed during the subsequent cycles and the conversion Co(OH)$_2$→CoOOH becomes prevailing ($E^0=-0.156$ V) with almost no change in mass (Eq. 5), what is in agreement with the experimental observations.

capacitance of the nanostructured sample was up to five times higher when compared to that of a mechanically abraded cobalt surface (with emery paper, grade 2500). This difference is caused by much higher actual surface area of the fiber-modified surface. Another important result is that the sulfide-containing sample exhibited an enhanced capacity up to three times ($C \approx 0.09$ F cm^{-2}) when compared to the sulfide-free counterpart.

Specific capacitance value is usually expressed as per 1 g of electroactive material. This is well reasoned when studying electroactive materials formed on foreign substrates which are frequently assumed to be electrochemically inert ones, for instance, $Co(OH)_2$ on stainless steel [22] or CoS_x on nickel [25–27]. In our case, however, the "per gram" approach has some specific features and has not to be straightforward adopted. The cobalt hydroxide is formed in situ on the parent metal, which is electrochemically active and any anodic polarization event leads to hydroxide formation until it reaches a limiting mass (EQCM measurements, Fig. 4). While only some part (most probably outer area) of the product is redox active, the conventional "per gram" calculation would involve both the active and the "ballast" parts reducing the calculated capacitance performance. It is also important that the EQCM measurements determine mainly the oxygen mass attached to the substrate (as O^{2-} or OH^-) not taking into account the metal mass (Co^{2+}), thus, to calculate the product exact mass, its exact chemical composition has to be known.

According to Fig. 4, the entire increase in the electrode mass after ten cycles is $\Delta m \approx 70$ µg cm^{-2} which is due mainly to O^{2-} attachment (the contribution by proton is relatively small). Assuming $Co(OH)_2$ as a product, one can calculate the mass of hydroxide $\Delta m \approx 117$ µg cm^{-2}. Taking into account the charge passed during the polarization cycle and the width of the polarization interval, we obtained capacity value $C=256$ F per 1 g of totally developed Co$(OH)_2$, i.e., not entirely electroactive one. Thus, a question arises which part of the entire structure participated in the capacitive process?

When comparing the electricity quantity of the hydroxide layer formation (Q_1, Fig. 5) with that responsible for the capacitance (Q_2 or Q_3, insertion in the figure), one can be seen that the quantities differ about one order of magnitude. So, the value $Q_1=0.565$ A s^{-1} was calculated for the two-electron transition $Co \rightarrow Co(II)$ leading to hydroxide formation, and $Q_2 \sim Q_3 \sim 0.055$ A s^{-1} was found for the equally two-electron transition process $Co(II) \rightarrow Co(III) \rightarrow Co(IV)$, which determines the capacitance. Such difference implies that only some 10% of the entire hydroxide structure took part in the capacitive process. Thus, the capacitance value calculated per one electroactive gram of hydroxide will be close to the limit 2,421 F g^{-1}, which predicts the Faraday's

law for $Co(OH)_2$ under our experimental conditions. This implies reliability of the active part estimation of entire Co$(OH)_2$ mass taken from EQCM data.

The voltammetric measurements (Fig. 6) have shown that sulfide-containing sample exhibited enhanced electrochemical capacity performance, which was up to three times higher when compared to the sulfide-free counterpart. Such effect could be explained in terms of sulfide-assisted development of actual surface area of hydroxide. The authors of [27] studied chemically prepared cobalt sulfide in alkaline medium and pointed out that cobalt sulfide exhibited poor electrochemical capacitance during the first polarization cycles [27]. With prolonged polarization, however, the capacitance increased up to impressive value 910 F g^{-1}. The reason of superior capacitance performance is attributed to electrochemical sulfide transformation to hydroxide in some outer area, which has distinctively highly-developed surface. The electrochemical reconstruction of the hydroxide should be responsible for good energy storage rather than the sulfide itself. In our experiments, the sulfide–hydroxide structure was deposited electrochemically; thus, it is quite possible that the mentioned sulfide–hydroxide transformation took place already in the preparation stage. Indeed, even the first polarization cycle measurement indicated superior electrochemical capacitance. Further research is needed to elucidate exact charge storage mechanism in cobalt sulfide structures.

Conclusions

The electrochemical capacitance values of the oxide/hydroxide formed on the cobalt nanofiber substrate were found to be up to five times higher when compared to those of conventional cobalt. The sulfide incorporation led to further enhancement of capacitance by up to three times. The electrode mass increase during anodic polarization was due mainly to the charge transfer $Co \rightarrow Co(II)$ with formation of $Co(OH)_2$. The transitions, which determine the pseudocapacitance behavior $Co(II) \rightarrow Co(III) \rightarrow Co(IV)$, do not cause remarkable electrode mass changes.

Charge quantity calculations showed that some 10% of the entire developed hydroxide took part in the capacitive process. This result was in agreement with a capacitance limit predicted by Faraday's law.

References

1. Conway BE (1999) In: electrochemical supercapacitors—scientific fundamentals and technological applications. Kluwer Academic Publisher, New York
2. Burke AJ (2000) J Power Sources 91:37
3. Zheng JP, Cygan PJ, Jow TR (1995) J Electrochem Soc 142:2699

4. Chen Z, Merryman SA (1999) In: Proceedings of the 9th International Seminar on Double-layer Capacitors and Similar Energy Storage Devices, Deerfield Beach
5. Sugimoto W, Iwata H, Yasunaga Y, Murakami Y, Takasu Y (2003) Angew Chem Int 42:4092
6. Hughes M, Chen GZ, Shaffer MSP, Fray DJ, Windle AH (2002) Chem Mater 14:1610
7. Srinivasan V, Weidner JW (1997) J Electrochem Soc 144:L210
8. Lin C, Ritter JA, Popov BN (1998) J Electrochem Soc 145:4097
9. Jayashree RS, Kamath PV (1999) J Mater Chem 9:961
10. Liu T-C, Pell WG, Conway BE (1999) Electrochim Acta 44:2829
11. Srinivasan V, Weidner JW (2002) J Power Sources 108:115
12. Shindle VR, Mahadik SB, Gujar TP, Lokhande CD (2006) Appl Surf Sci 252:7487
13. Kim HK, Seong TY, Lim JH, Cho WI, Yoon YS (2001) J Power Sources 102:167
14. Hu CC, Hsu TY (2008) Electrochim Acta 53:2386
15. Kandalkar SG, Gunjakar JL, Lokhande CD (2008) Appl Surf Sci 254:5540
16. Cao L, Xu F, Liang Y-Y, Li HL (2004) Adv Mater 16:1853
17. Cao L, Lu M, Li H-L (2005) J Electrochem Soc 152:A871
18. Hosono E, Fujihara S, Honma I, Ichihara M, Zhou H (2006) J Power Sources 158:779
19. Nguyen Q, Wang L, Lu GM (2007) Int J Nanotechnol 4:588
20. Zhou W-J, Zhao D-D, Xu MW, Xu C-L, Li HL (2008) Electrochim Acta 53:7210
21. Yuan CZ, Zhang XG, Gao B, Li J (2007) Mater Chem Phys 101:148
22. Gupta V, Kusahara T, Toyama H, Gupta S, Miura N (2007) Electrochem Commun 9:2315
23. Lichušina S, Chodosovskaja A, Seleskis A, Leinartas K, Miečinskas P, Juzeliūnas E (2008) Chemija 19:7
24. Wang J, Ng SH, Wang GX, Chen J, Zhao L, Chen Y, Liu HK (2006) J Power Sources 159:287
25. Tao F, Zhao Y-Q, Zhang G-Q, Li H-L (2007) Electrochem Commun 9:1282
26. Bao S-J, Li CM, Guo C-X, Qiao Y (2008) J Power Sources 180:676
27. Yuan C, Gao B, Su L, Chen L, Zhang X (2009) J Electrochem Soc 156:A199
28. Juzeliūnas E, Lichušina S Patent of the Republic of Lithuania No. 5481 26.03.2008
29. Burke LD, Lyons ME, Murphy OJ (1982) J Electroanal Chem 132:247
30. Bell WK, Toni JE (1971) J Electroanal Chem 31:63